

---

# Molecular Gas in Nearby Dwarf Galaxies: Single Dish and Interferometric Results

Alberto D. Bolatto<sup>1</sup>, Adam Leroy<sup>1</sup>, Josh D. Simon<sup>1</sup>, Leo Blitz<sup>1</sup>, and Fabian Walter<sup>2</sup>

<sup>1</sup> Department of Astronomy, University of California at Berkeley  
[bolatto@astro.berkeley.edu](mailto:bolatto@astro.berkeley.edu)

<sup>2</sup> National Radio Astronomy Observatory

## 1 Introduction: The MIDGET Survey

During the past two years we have undertaken a systematic millimeter-wave survey of molecular gas in a sample of 150 nearby, northern dwarf galaxies with IRAS emission. We have called this survey MIDGET (Millimeter Interferometry of Dwarf Galaxies). MIDGET has two parts: a single-dish search for CO done at the UASO Kitt Peak 12m telescope (Leroy et al., in preparation), and an interferometric follow-up of the galaxies with strong CO emission carried out at the Berkeley–Illinois–Maryland Array (BIMA). The single-dish survey targeted the centers of northern galaxies that are nearby ( $V_{\text{LSR}} \leq 1000 \text{ km s}^{-1}$ ), of small mass (HI linewidths  $W_{20} \leq 200 \text{ km s}^{-1}$ ), compact in size, and detected by IRAS. The single-dish observations were very successful, finding 41 new CO emitters and more than doubling the number of previously known CO sources within the defined sample. The typical  $1\sigma$  sensitivity attained was  $\sim 0.2 \text{ K km s}^{-1}$ . Carbon monoxide emission was detected in galaxies with  $12 + \log([\text{O}/\text{H}]) \sim 7.9 - 8.5$ , a metallicity regime similar to that of the Magellanic Clouds. We are using these data to address several questions related to molecular cloud and star formation in these objects. This paper concentrates on the issue of how CO traces molecular gas as a function of heavy element abundance  $Z$ .

## 2 Does the $X_{\text{CO}}$ Factor Depend Strongly on Metallicity?

Measuring the amount of molecular hydrogen present using CO observations requires assuming a CO-to-H<sub>2</sub> conversion factor  $X_{\text{CO}} = N(\text{H}_2) / \int I(\text{CO}) dv$  (e.g., Sanders, Solomon, & Scoville 1984). This factor will be a product of abundance, excitation, and cloud structure averaged over a large area. The theoretical expectation is that the  $X_{\text{CO}}$  factor will depend on the local properties of the interstellar medium (ISM) such as volume density, temperature,

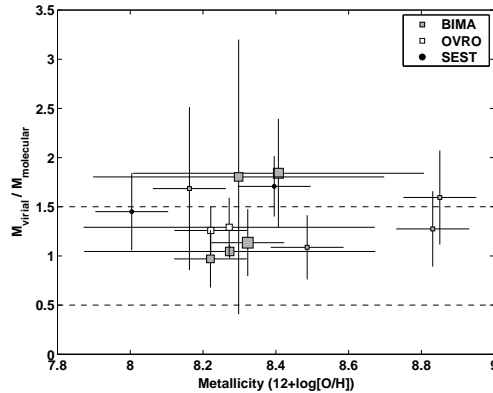


**Fig. 1.** Virial CO-to-H<sub>2</sub> conversion factor as a function of metallicity, normalized to the Galactic value. Each point represents the average of the ratio of virial to molecular mass for all the GMCs analyzed in one galaxy, with the molecular mass computed using the integrated CO intensity and the Galactic X<sub>CO</sub> factor. Symbol color identifies the telescopes used for the measurements, while size is proportional to the spatial resolution attained in the observations. The data include clouds in M 33, the SMC (N83/N84), the LMC (N159/N160), IC 10, NGC 2976, NGC 3077, NGC 4214, NGC 4449, and NGC 4605.

and metallicity. The dependence of X<sub>CO</sub> on metallicity  $Z$  remains a point of contention. Some authors find X<sub>CO</sub> strongly increasing for decreasing  $Z$  (e.g., Wilson 1995; Israel 1997), while other, recent work finds no apparent trend (e.g., Rosolowsky et al. 2003).

We have used the interferometric data to measure the properties of individual molecular clouds (size, velocity dispersion, CO luminosity) in dwarf galaxies where we can accurately derive virial masses. For these measurements we have developed a robust algorithm called **CLOUDALYZE**, which uses moments of the intensity distribution computed over connected regions of the datacube as a function of a threshold intensity (Bolatto et al. 2003). These moments, adequately corrected to account for angular resolution and signal-to-noise effects, are then used to compute the size and velocity dispersion of a cloud, thus measuring its virial mass. In designing this experiment we have explicitly tried to avoid problems common in some extragalactic X<sub>CO</sub> determinations found in the literature. In particular, we deconvolved the beam from our cloud size estimates and we avoided unresolved clouds. Another potentially complicating effect is cloud blending in velocity space. In poor signal-to-noise data, emission from two or more clouds may be confused and assigned to only one entity. Because the velocity dispersion is squared to compute the virial mass, velocity cloud blending can introduce large errors that overestimate virial masses.

Figure 1 shows the ratio of virial mass to molecular mass traced by CO using the Galactic conversion factor ( $X_{CO} = 2 \times 10^{20} \text{ cm}^{-3}/\text{K km s}^{-1}$ ) found by

using CLOUDALYZE on several extragalactic GMCs. These include observations performed by BIMA and OVRO, as well as SEST observations of regions in the LMC and SMC. This plot shows that resolved extragalactic GMCs have an approximately Galactic CO-to-H<sub>2</sub> conversion factor regardless of metallicity. The offset from  $M_{virial}/M_{mol} = 1$  is probably due to the algorithm, which has not been scaled to produce  $M_{virial} = M_{mol}$  in Galactic GMCs (e.g.,  $M_{virial}/M_{mol} = 1.5$  in the Rosette GMC).

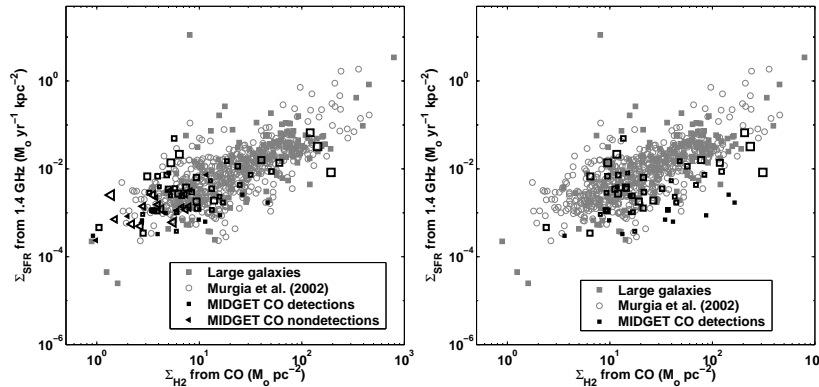


**Fig. 2.** (a) Surface density of star formation rate versus surface density of molecular gas, for the central pointings of galaxies in the FCRAO catalog (gray symbols), the sample from Murgia et al. (2002) which includes all FCRAO pointings (gray circles), and the MIDGET galaxies (black symbols). Triangles indicate CO upper limits. The SFR was obtained from the 1.4 GHz radio continuum NVSS images, which have a resolution matched to that of the CO observations. The column density of molecular gas was obtained from the CO using the Galactic conversion factor. (b) Same plot as (a), but the MIDGET points now show the effects of applying a metallicity correction to  $X_{CO}$  such as the one by Wilson (1995). The symbol sizes for the MIDGET points are proportional to metallicity.

Is there any evidence for a constant CO-to-H<sub>2</sub> conversion factor apart from the virial arguments made above? Using NVSS radio continuum images and following Murgia et al. (2002) we can readily obtain the star formation rate (SFR) in the central regions of these galaxies with a beam size matched to the single-dish CO measurement. Figure 2a shows the surface density of SFR against that of molecular gas. In this diagram, dwarf galaxies occupy the same locus as more massive galaxies. If the Galactic  $X_{CO}$  factor used to obtain  $\Sigma_{H_2}$  were systematically underestimating the amount of H<sub>2</sub> available for star formation in dwarf galaxies then their points would be displaced to the left of those of bigger galaxies and they are not. In fact, attempts to correct  $X_{CO}$  for metallicity effects (using the metallicities inferred from  $M_B$ ; Richer & McCall 1995) such as that in Figure 2b clearly destroy the agreement and appear to

overestimate the surface density of molecular gas for a given star formation rate.

It is possible that the radio continuum emission from dwarf galaxies might be less bright for a given star formation rate — perhaps as a result of lower magnetic field strength in these galaxies. This effect could collude with a metallicity-dependent  $X_{\text{CO}}$  factor to keep dwarf galaxies on the same locus as the large galaxies despite the application of an incorrect  $X_{\text{CO}}$  factor. We have looked into this possibility. We find that small galaxies with  $V_{\text{rot}} \sim 70 - 110 \text{ km s}^{-1}$  fall in the same radio continuum to far infrared correlation as the larger galaxies: in this regard the radio continuum seems to be as good a tracer of SFR as the far infrared for these objects. For this alternative explanation to work, there needs to be almost perfect cancellation between the increase in  $X_{\text{CO}}$  and the reduction in the SFR measured by the radio continuum.

### 3 Conclusions

Using virial mass arguments, we showed that the  $X_{\text{CO}}$  factor measured in resolved extragalactic GMCs is not strongly dependent on metallicity. Using the correlation between radio continuum and molecular gas, we argued that a Galactic CO-to-H<sub>2</sub> conversion factor appears to explain the observed SFR in small galaxies as well as in large galaxies. Thus, at least for the molecular gas relevant to star formation processes,  $X_{\text{CO}}$  in these metal-poor environments appears to be approximately Galactic regardless of metallicity.

A few cautionary statements are in order. First, and perhaps more importantly, this result does not mean that  $X_{\text{CO}} = 1$  in every conceivable environment. We are only able to obtain virial mass estimates for very special objects, the brightest extragalactic GMCs. This result thus may have little bearing on the CO-to-H<sub>2</sub> conversion factor over an entire galaxy, except perhaps that molecular gas with high  $X_{\text{CO}}$  does not appear to be important for star formation. Second, the physics relating the FIR and radio continuum emission to the star formation rate are poorly understood. Therefore it is possible that other effects come into play that cancel an increase in  $X_{\text{CO}}$ . This cancellation, however, needs to be almost perfect. Finally, to properly make quantitative arguments such as those in Figure 2b it is desirable to have direct metallicity measurements on a large sample of dwarf galaxies where CO is observed. We have used a rather indirect estimator of metallicity with a large intrinsic scatter ( $M_B$ ), because no other data are available.

### References

1. Bolatto, A. D., Leroy, A., Israel, F. P., & Jackson, J. M. 2003, ApJ, 595, 167
2. Israel, F. P. 1997, A&A, 328, 471
3. Murgia, M., Crapsi, A., Moscadelli, L., & Gregorini, L. 2002, A&A, 385, 412

4. Richer, M. G. & McCall, M. L. 1995, *ApJ*, 445, 642
5. Rosolowsky, E., Plambeck, D., Engargiola, G., & Blitz, L. 2003, *ApJ*, in press
6. Sanders, D. B., Solomon, P. M., & Scoville, N. Z. 1984, *ApJ*, 276, 182
7. Wilson, C. D. 1995, *ApJ*, 448, L97.